Noncontact Laser-Induced Ultrasound for Composites Inspection: Approaches for Material Discontinuity Visualization

L. MAIO[1], Z. WU[2], P. POTLURI[1] and M. D. TODD[2]

Abstract

Pulsed laser techniques enable non-contact generation of ultrasound in composite materials and can provide full-wavefield data. Nonetheless, since a pulsed laser provides a broadband excitation of acoustic waves, the resulting field contains both the dominant propagating modes and the weaker signals caused by interactions with possible internal defects such as delaminations. Hence, proper analyses of wavefields become essential to reveal subtle phenomena that can be masked by the primary wavefronts. In this study, the Singular Value Decomposition is applied to the measured wavefield to effectively separate and suppress the main wave components, whereas time-integrated maps are computed to enhance the discontinuity visualization. Experimental results from a composite plate with artificial interlaminar defect demonstrate that the adopted processing approaches improve defect contrast and facilitate more accurate localization of subsurface delaminations.

Keywords pulsed laser, ultrasonic wavefield, matrix factorization, guided waves, time-integrated maps, composite

1. Introduction

Composite materials, such as carbon fiber-reinforced polymers (CFRPs), are widely used in aerospace, automotive, and civil infrastructure due to their excellent mechanical properties and low weight. Despite their advantages, they are vulnerable to internal flaws such as delaminations, which significantly degrade structural performance and are challenging to detect with conventional nondestructive testing (NDT) methods [1,2].

Laser ultrasonic (LU) technology has emerged as a promising non-contact method for NDT of composite structures. It offers flexibility, high spatial resolution, and the ability to operate on complex geometries without couplants [3,4]. Such a technique typically involves a pulsed laser (e.g.,Nd:YAG) that generates ultrasonic waves via thermoelastic or ablative effects and a sensing system based on fixed transducers or laser Doppler vibrometer (LDV) for detecting surface displacements [5-7]. Numerous studies have confirmed the viability of LU method for detecting delaminations, impact damage, and other subsurface anomalies in CFRPs [8-10].

One powerful feature of LU technology is its compatibility with full wavefield imaging. When combined with scanning LDV, it enables visualization of Lamb wave propagation and interaction with defects [11, 12]. Lamb waves, which are multimodal and dispersive, are especially useful in thin composite plates where they can probe through the thickness and reflect damage-sensitive behaviour [13–15]. Alternatively, an important physical concept supporting LU analysis is the reciprocity principle in linear elastodynamics. This principle allows the measured wavefield to be interpreted as a response from a virtual source at the transducer location, propagating through the scanned surface

[1]Department of Materials, University of Manchester, Manchester, UK
[2]Department of Structural Engineering, University of California San Diego, La Jolla, CA
leandro.maio@manchester.ac.uk

points as receivers [16,17]. This reversed-source view is particularly useful for damage localization, as scattered wavefields can be attributed to specific features in the material [18, 19].
To enhance the visibility of such scattered waves, especially in the presence of strong direct waves, filtering approaches should be applied to wavefield data. A mathematical tool useful for this purpose is the Singular Value Decomposition (SVD), which decomposes the wavefield into a set of orthogonal modes ranked by their significance. Previous studies have demonstrated the utility of SVD in seismic imaging, medical ultrasound, and other areas of wavefield processing, showing that it can significantly improve defect detectability. Nonetheless, its application to laser ultrasonic inspection of composite materials, particularly for delamination detection, remains an active area of research.
This paper investigates the application of SVD-based wavefield filtering to laser ultrasonic data obtained from composite plates. The objective is to attenuate the dominant wave components, in order to amplify signals from delaminations, and improve the overall defect visibility. Moreover, L_1-norm is adopted to collapse the temporal dimension of wave propagation data into a single spatial snapshot, revealing cumulative amplitude distribution. The remainder of the paper is organized as follows: section 2 details the SVD-based processing methodology and the use of time-integrated maps; section 3 describes the experimental setup and data acquisition process; section 4 presents experimental results and analysis; last section concludes the paper with comments and future perspectives.

2. Methodology

The Singular Value Decomposition (SVD) is a fundamental matrix factorization technique that decomposes any matrix in three matrices. Consequently, in order to apply the technique, the 3D wavefield data $\boldsymbol{W}(x,y,t)$ are reshaped into a 2D matrix $\boldsymbol{W}_r \in R^{(x\times y)\times t}$, with each row corresponding to a spatial location and each column to a time point. SVD is applied as:

$$\boldsymbol{W}_r = \mathbf{U}\boldsymbol{\Sigma}\mathbf{V}^T \tag{1}$$

where $\mathbf{U} \in R^{(xy)\times(xy)}$ and $\mathbf{V} \in R^{t\times t}$ contain orthonormal spatial and temporal modes respectively, while $\boldsymbol{\Sigma} \in R^{(xy)\times t}$ is a diagonal matrix of singular values. Specifically, $\mathbf{U}$ is an orthogonal matrix (whose columns are called the left singular vectors of $\boldsymbol{W}_r$) that contains orthonormal spatial modes. $\boldsymbol{\Sigma} \in R^{(xy)\times t}$ is a diagonal matrix with nonnegative real numbers on the diagonal, known as the *singular values* of $\boldsymbol{W}_r$. These numbers are usually arranged in descending order or sorted by energy content. $\mathbf{V}$ (or $\mathbf{V}^T$ in the decomposition) is an orthogonal matrix (whose columns are called the right singular vectors of $\boldsymbol{W}_r$) that contains temporal modes. The singular values in $\boldsymbol{\Sigma}$ indicate the "energy" or importance of each corresponding singular vector. Larger singular values represent directions (or modes) in which the data has a significant amount of variation. Conversely, smaller singular values are often associated with less significant features, sometimes even noise. The highest singular value corresponds to the dominant wavefront, usually the S_0 and A_0 mode. By removing the dominant modes, the previous equation becomes:

$$\boldsymbol{W}_{filtered} = \mathbf{U}\boldsymbol{\Sigma}_{filtered}\mathbf{V}^T \tag{2}$$

where $\boldsymbol{W}_{filtered}$ is the residual wavefield and $\boldsymbol{\Sigma}_{filtered}$ is given by:

$$\boldsymbol{\Sigma}_{filtered} = \boldsymbol{\Sigma} - \sum_{i=1}^{p} \sigma_i \mathbf{u}_i \mathbf{v}_i^T \tag{3}$$

with σ_i is the *i*-th singular value of the data matrix (singular values are ordered from largest to smallest: $\sigma_1 \geq \sigma_2 \geq \sigma_3 \geq .. \geq 0$) indicating the strength (energy) of the *i*-th mode, $\mathbf{u}_i$ is the *i*-th left singular vector, representing a spatial pattern, $\mathbf{v}_i$ is the *i*-th right singular vector, representing a temporal pattern and *p* is the number of retained dominant modes. More simply, removing (zero out) the dominant modes involves setting $\sigma_i = 0$ for the top singular values (modes), effectively subtracting those large-scale features:

$$\mathbf{\Sigma}_{filtered} = diag(\underbrace{0,...,0}_{p\ times}, \sigma_{p+1}, \sigma_{p+2}, ..) \tag{4}$$

Reconstructing the matrix with this modified $\mathbf{\Sigma}_{filtered}$ results in a filtered version of the wavefield, $\boldsymbol{W}_{filtered}$. This filtered matrix emphasizes subtle details through the removal of the strong, coherent background due to the main wave. In wavefield filtering applications, the dominant (largest) singular values are often associated with the primary signal components (like a strong propagating wave). In contrast, the smaller singular value components may capture secondary features (like scattering due to a delamination) or noise. By zeroing out certain singular values, unwanted parts of the signal are suppressed preserving the others. In order to define the number of singular modes to remove, an energy criterion can be set for the purpose. Since singular values indicate the contribution of each mode to the overall energy of the wavefield, the cumulative energy captured by the leading modes can be exploited for the purpose. Specifically, the modes can be retained or removed until a specified percentage (e.g., 90–95%) of the total energy is accounted for by the dominant components. Let σ_i be the singular values, the energy fraction for mode is calculated as follows:

$$E_i = \frac{\sigma_i}{\sum_j \sigma_j} \tag{5}$$

Afterwards, a threshold needs to be set such as a cumulative energy of 95%, herein adopted to improve the visibility of defects. The threshold separates the modes likely representing the primary wave from those that might contain the subtle features to be highlighted.

Another useful tool in wavefield analysis is represented by the time-integrated maps (TIMs) based on the norms like L_1 (absolute amplitude) and L_2 (energy) to process the data. They capture how wave phenomena accumulate over time, highlighting persistent scattering, modes, discontinuities. Specifically, wavefields are recorded over a long enough time window in order to allow ultrasound to propagate over the entire region of interest. Consequently, at some spatial locations, acquired signals enclose not only the direct wave from the source but reflections, mode-converted signals from boundaries, entrapped energy, and other material or geometrical features of the specimen. Therefore, an image based on energy or an equivalent quantity and built over a large time window, includes all of these contributions. Moreover, by integrating over a suitable time window, the contribution of direct arrivals can be minimized, emphasizing later phenomena. In this framework, using the absolute amplitude instead of squared amplitude, when constructing a TIM, can offer unique advantages in highlighting energy trapped in delaminations. Given a recorded wavefield $w(x,y,t)$ over time $t \in [t_0, t_1]$, the L_1-norm-based time-integrated map is defined as:

$$E_w(x,y) = \int_{t_0}^{t_1} |w(x,y,t)| dt \tag{6}$$

Therefore, it can be evaluated by summing up the amplitudes (in absolute value) of the time-series wave signal collected at each grid point. Consequently, the norm measures cumulative amplitude magnitude, not the energy. While delaminations trap energy through multiple internal reflections, the L_2 norm disproportionately weights high peaks, whereas L_1 captures repeated moderate amplitudes resulting from trapped waves. The linear summation is less skewed by noise or measurement spikes, this leads to cleaner, sparser maps that better isolate delamination zones.

3. Experimental setup

The laser ultrasonic interrogation system adopted for the experiments comprises a laser scanning system incorporated with signal-conditioning and data acquisition modules, an ultrasonic resonant sensor, and a computer used for signal processing and operation control. Such a system presents a 2D scanning mirror and a diode-pumped solid-state Q-switched Nd:YAG laser. The Q-switched laser is composed of a controller and a laser head with an output beam of 527-nm wavelength and pulse repetition rates of single-shot up to 1 kHz. The mirror is used to synchronize the two-axis galvanometer scanner with the Q-switched laser to manoeuvre the impinging point rapidly at a pulse repetition rate with predefined two-dimensional space coordinates. The described system can perform a scanning process based on a programmable scanning path such as a traditional raster or a circle. In the carried out experiments, the scanned region covers a two-dimensional grid, 100 mm x 100 mm, on the composite plate surface with scanning step 0.5 mm resulting in 40000 grid points. Figure 1(a) provides a view of the whole experimental setup, with the laser system in the foreground and the test article in the background. The specimen is a symmetric, quasi-isotropic graphite/epoxy laminate with dimensions of 600 x 600 x 1.6 mm³ and a stacking sequence of $[+45/-45/0/90]_s$ [24,25]. A circular polytetrafluoroethylene film, measuring 15 mm in diameter, was included during the layup process at the second interface (i.e. between the 2nd and 3rd ply, where eighth ply is in front of the laser head) to replicate an artificial disbond. A circular crown was detected around the artificial delamination by Olympus OmniScan SX equipped with phased array probe, indicating that the effective diameter of the artificial delamination is about 20 mm [24]. This is centred with the scanning grid.

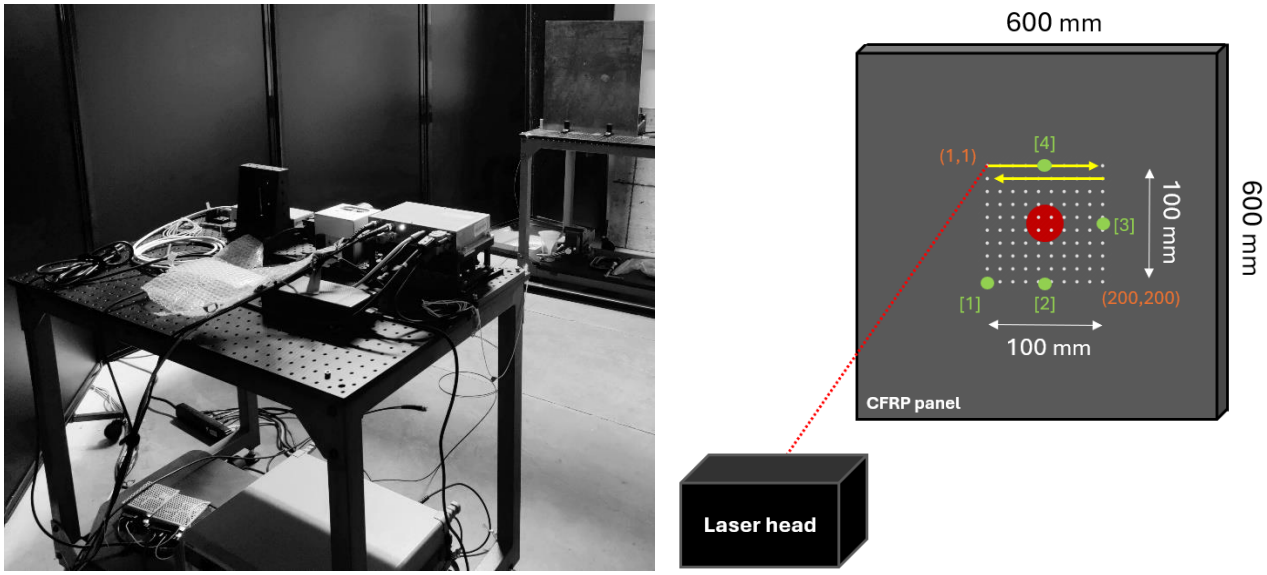

(a) (b)

Figure 1 – (a) Experimental setup of the laser head mounted on the scanner in front of the test article. (b) Schematic representation of the laminated panel with defect (red disk), subsequent transducer positions (green disks with numbers), and measuring grid (white dots). The laser beam (dotted red line) aims at the first scanning point and moves according to the raster scanner path (yellow arrows).

During the scanning process, the laser pulse impinges at a scan point and ultrasound is generated through thermoelastic effect. The ultrasonic waves are then sensed by the resonant contact transducer, exhibiting a strong response at 120 kHz. The signal is sampled at 10 MHz for 200 μs through the digital acquisition module triggered by the controller after the laser pulse is emitted. Lastly, all digitized ultrasonics are stored in a computer in the form of a three-dimensional matrix. Signal acquisition over the entire scanning area is repeated according to the different positions of the single fixed transducer. A schematic view of the scanned panel is given in Figure 1(b), where the defect, the four distinct transducer locations, and the measurement area are highlighted.
Under the assumption of linear, reciprocal media, the data acquired from a fixed transducer with a moving source (scanning the surface) can be interpreted as a time history of a virtual wave being emitted from the transducer and received at every scanned point [16,17]. This reciprocity-based perspective effectively reverses the propagation direction, allowing the reconstruction of the wavefield to be analysed.

4. Results and discussion

Figure 2 shows four pairs of maps computed using the full time window of 200 μs and corresponding to the four arrangements of the fixed transducer. Specifically, the maps on the left correspond to the normalized TIMs of the unfiltered wavefield, whereas the ones on the right are the normalized TIMs of the wavefield filtered through the SVD factorization. The time window is selected to ensure that the primary incident waves from the source transducer travel through the whole scan area so that the entire region of interest is interrogated.
First, all the TIMs of unfiltered wavefields on the left, in Figure 2, show that the angular pattern of the incident wavefield is not uniform with lowest amplitude in the -45° directions and highest at +45°, direction of the outermost ply. These variations can be attributed to the specimen orthotropy and layup. Moreover, the transducer appears as an anomaly of high amplitude as well as the delamination, because of waves trapping within it [26]. In fact, each location on the panel is stimulated and interrogated by multiple waves which affect the transducer from different directions, and thus even the delaminated region, characterized by two distinct thicknesses of material, that directly receives energy from the laser. The noisy background is typical of laser-based data and depends even on the surface quality impinged by the laser. Indeed, in most maps it is possible to notice the presence of a background square due to adhesive residues from a previous application of reflective tape for LDV measurements. As for the residual wavefield characterizing all the maps on the right in Figure 2, this clearly shows the energy radiating from delaminated regions, consistent with the artificial defect in the composite [24,25]. The residual wavefield attenuates the primary incident waves and the transducer contribution, but enhances the visibility of the discontinuity inside the panel. However, to reduce noise and enhance the visibility of significant energy concentrations, median filtering can be a helpful step in preprocessing the TIM of a wavefield. It is effective at removing impulsive noise from images, which can help clarify regions of high or low energy. Furthermore, unlike linear filters, 2D median filtering preserves edges and boundaries better, which can be important for accurately identifying concentrated energy regions. In Figure 3(a), each pixel contains the median value in a 3-by-3 neighbourhood around the corresponding pixel of TIM depicted in Figure 2(h). By reducing small-scale fluctuations and noise, this approach can make the larger, more meaningful energy concentrations stand out more clearly.
Finally, as shown in Figure 3(b), thresholding the energy map through a factor of the maximum energy allows highlighting areas of high accumulated energy and thus detecting the trapped energy region corresponding to the delamination.

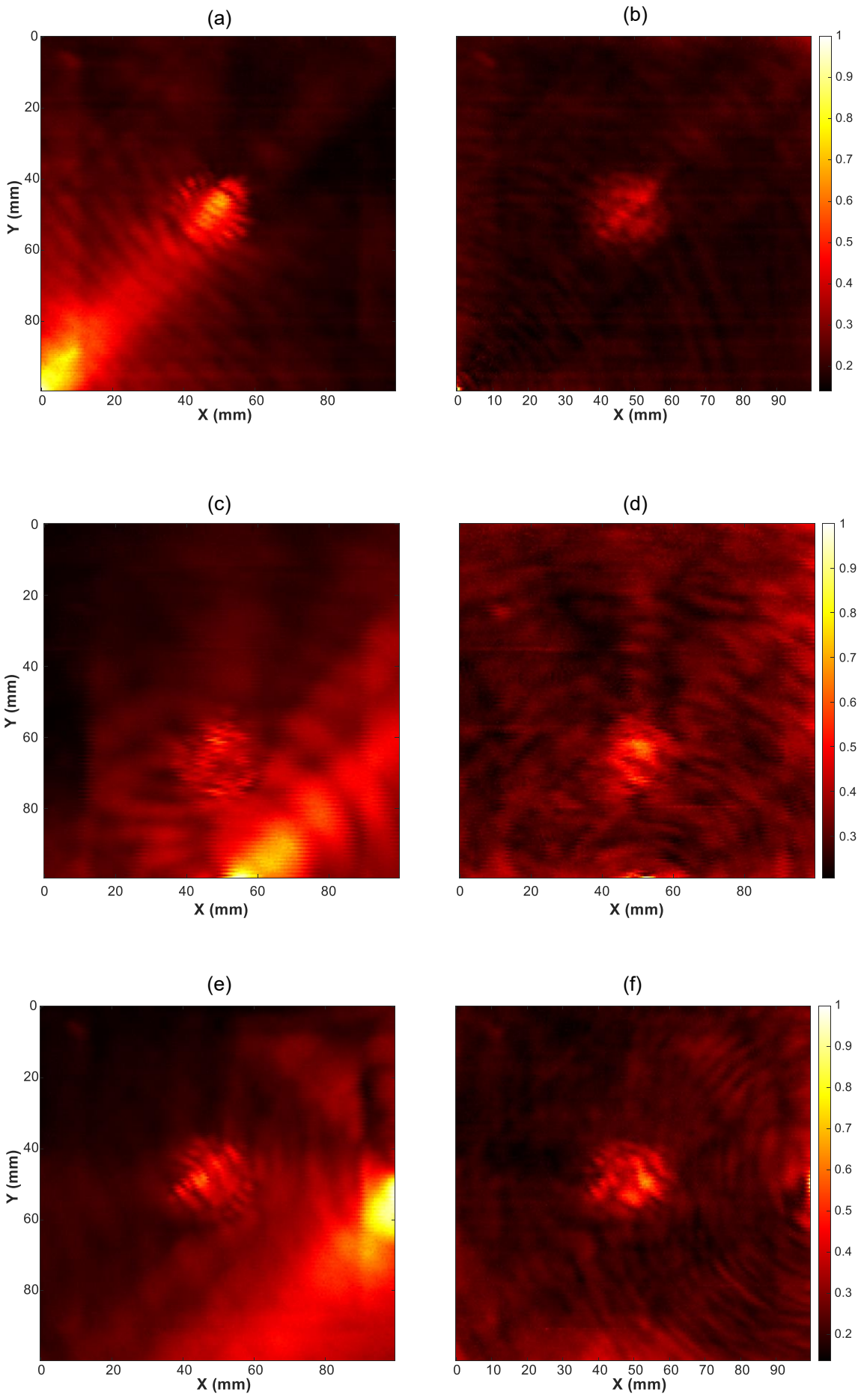
(a)
(b)
(c)
(d)
(e)
(f)
Y (mm)
X (mm)
0
20
40
60
80
10
30
50
70
90
1
0.9
0.8
0.7
0.6
0.5
0.4
0.3
0.2

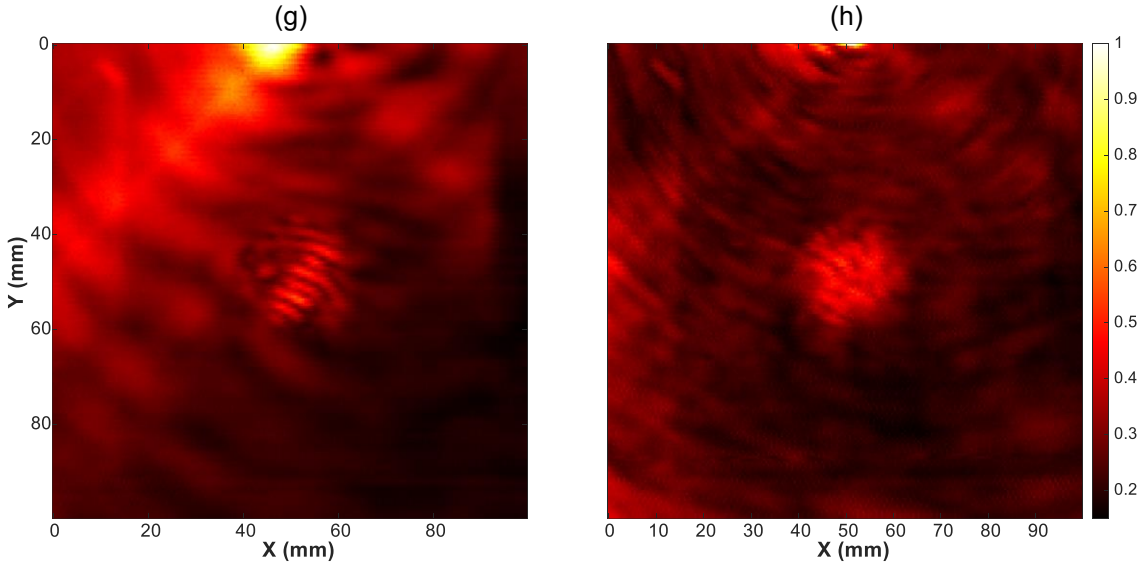

Figure 2 – (a) (c) (e) (g) normalized TIM of the unfiltered wavefield for the [1] [2] [3] [4] positions of the fixed transducer (see Figure 1(b)) respectively. (b) (d) (f) (h) normalized TIM of the filtered wavefield for the [1] [2] [3] [4] positions of the transducer.

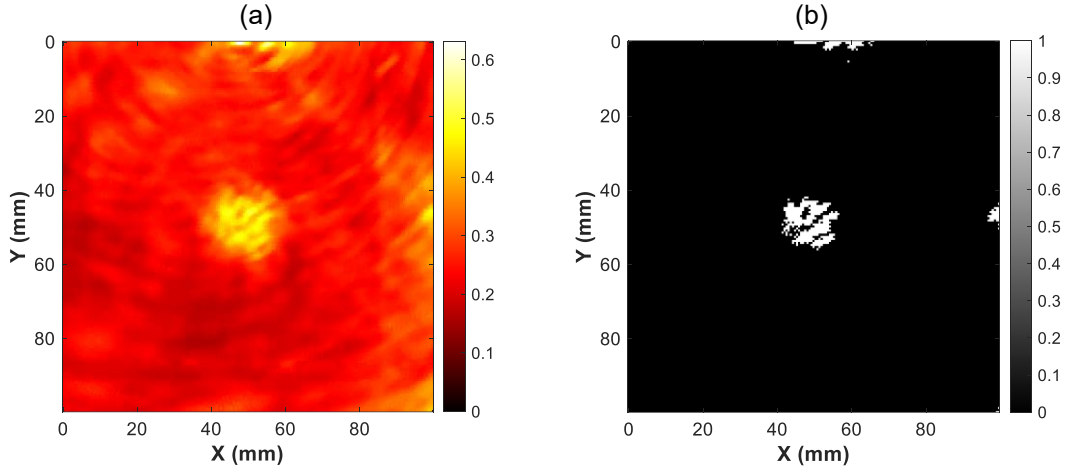

Figure 3 – Referring to [4] position of the transducer (see Figure 1(b)): (a) 2-D median filtering applied to the normalized TIM of the filtered wavefield (Figure 2(h)) and (b) detected discontinuity by thresholding energy map for [4] position of the transducer.

5. Conclusion

This work integrates laser-generated guided waves with SVD, TIM and image-filtering algorithms to enhance the visibility of delaminations in CFRP composites. The approach enables full wavefield capture without contact or coupling agents, leverages the reciprocity principle to reinterpret scanning data as virtual-source wavefields and applies SVD to suppress dominant wave modes and L_1-norm-based time-integrated map to isolate damage-related effects. The experimental validation shows that the adopted methodology clearly highlights delamination location with accuracy, proving worthy of consideration for non-destructive evaluation of advanced composite structures. Future work will focus on extending this methodology to complex geometries, curved surfaces, thicker structures and integrating machine learning for automated damage classification.

References

1. Scruby, C.B., & Drain, L.E. (1990). *Laser Ultrasonics: Techniques and Applications*. Adam Hilger.
2. Dewhurst, R.J., Hutchins, D.A., & Palmer, S.B. (1981). Laser generation as a standard acoustic source in metals. *Applied Physics Letters*, 38(9), 677–679.
3. Palmer, S.B., & Hutchins, D.A. (1994). Laser-based ultrasound: generation and detection of ultrasound using lasers. *Ultrasonics*, 32(1), 17–28.
4. Michaels, J.E., & Michaels, T.E. (2005). Guided wave signal processing and image fusion for in situ damage localization in plates. *Wave Motion*, 42(4), 215–228.
5. Rose, J.L. (2014). *Ultrasonic Guided Waves in Solid Media*. Cambridge University Press.
6. Flynn, E.B., & Johnson, J.A. (2010). Wavenumber filtering for detection of structural damage using laser ultrasonic guided waves. *NDT & E International*, 43(8), 642–651.
7. Li, S., Zhu, Y., Wang, H., & Xu, C. (2019). Laser ultrasonic testing of delamination in composite materials. *Nondestructive Testing*, 41(5), 1–5. https://doi.org/10.11973/wsjc201905001
8. Zhang, D., Li, H., Song, C., Zhou, X., Shen, S., Zhang, G., Yang, Y., & Wang, H. (2020). A new laser ultrasonic inspection method for detection of multiple delamination defects. *Materials*, 14(9), 2424.
9. Li, Q., Cheng, X., Wu, X., Lu, C., Zhang, H., & Shang, J. (2025). Study on laser ultrasonic testing mechanism of delamination defects in anisotropic curved CFRP. *Optical Engineering*, 64(1), 014101.
10. Lanza di Scalea, F., Rizzo, P., & Savoia, A. (2006). Localized inspection of composite plates by laser-generated Lamb waves. *Smart Materials and Structures*, 15(2), 493.
11. Wu, Z., & Giurgiutiu, V. (2014). Laser ultrasonic techniques for structural health monitoring of aerospace composite structures. *Sensors*, 14(7), 11643–11664.
12. Demma, A., Cawley, P., Lowe, M.J.S., & Rokhlin, S.I. (2005). The reflection of the fundamental Lamb modes from a part-through notch. *The Journal of the Acoustical Society of America*, 117(2), 753–764.
13. Alleyne, D.N., & Cawley, P. (1991). A two-dimensional Fourier transform method for the measurement of propagating multimode signals. *The Journal of the Acoustical Society of America*, 89(3), 1159–1168.
14. Zabel, V., Khorasani, M., & Ruzzene, M. (2018). Wavefield separation and damage imaging based on singular value decomposition. *Mechanical Systems and Signal Processing*, 102, 529–547.
15. Park, S., Lee, J., & Kim, Y. (2018). Non-contact ultrasonic inspection of impact damage in composite laminates by visualization of Lamb wave propagation. *Applied Sciences*, 9(1), 46.
16. Yan, Z., Wu, J., Li, X., & Hu, J. (2019). Damage imaging in composite plates using laser ultrasound and wavenumber filtering. *Composite Structures*, 223, 110970.
17. Sato, K., & Yamashita, T. (2015). Non-contact laser ultrasonic detection of delamination in CFRP laminates using guided waves. *NDT & E International*, 71, 12–18.
18. Raghavan, A., & Cesnik, C.E.S. (2007). Review of guided-wave structural health monitoring. *The Shock and Vibration Digest*, 39(2), 91–114.
19. Grédiac, M., Rizzo, P., & Sabatier, L. (2017). Ultrasonic guided waves for structural health monitoring: From fundamentals to applications. *Elsevier*.
20. Royer, D., & Dieulesaint, E. (2000). *Elastic Waves in Solids I: Free and Guided Propagation*. Springer.
21. Neogi, A., & Kumar, R. (2018). Detection of delamination using laser ultrasonic Lamb waves in composite laminates. *Composite Structures*, 184, 99–108.
22. Li, C., & Rose, J.L. (2014). Delamination detection and characterization in composite laminates by using guided ultrasonic waves. *Smart Materials and Structures*, 23(9), 095013.
23. Wu Z., Chong S. Y., Todd M. D. (2021). Laser ultrasonic imaging of wavefield spatial gradients for damage detection, Structural Health Monitoring, 20(3), 960-977.
24. Maio L., Memmolo V., Boccardi S., Meola C., Ricci F., Boffa N. D., Monaco E. (2016). Ultrasonic and IR Thermographic Detection of a Defect in a Multilayered Composite Plate, Procedia Engineering, 167, p. 71-79.
25. Maio L., Hervin F., Fromme P. (2020). Guided wave scattering analysis around a circular delamination in a quasi-isotropic fiber-composite laminate, Proceedings Volume 11381, Health Monitoring of Structural and Biological Systems XIV; 113810Q.
26. Ricci F., Mal A. K., Monaco E., Maio L., Boffa N. D., Di Palma M, Lecce L. (2014). Guided Waves in Layered Plate with Delaminations. EWSHM - 7th European Workshop on Structural Health Monitoring, IFFSTTAR, Inria, Université de Nantes, Nantes, France.